MOP as a Corrosion Inhibitor for Mild Steel in HCl Solution: A Comprehensive Study

A. F. Hamood[1], H. S. Aljibori [2], M. A. I. Al-Hamid [3], A. A. Alamiery [3, 4*], W. K. Al-Azzawi [5]

[1.] Production and Metallurgy Engineering, University of Technology, P.O. Box: 10001, Iraq

[2.] College of Engineering, University of Warith Al-Anbiyaa, Karbalaa, P.O. Box: 56001, Iraq

[3.] Energy and Renewable Energies Technology Center, University of Technology, P.O. Box: 10001, Iraq

[4.] Faculty of Engineering and Built Environment, Universiti Kebangsaan Malaysia, Bangi, Selangor, P.O. Box: 43600, Malaysia

[5.] Al-Farahidi University, Baghdad, P.O. Box: 10001, Iraq.

ABSTRACT

*C*orrosion of mild steel in aggressive environments such as HCl solution poses significant challenges across industries. This research explores the potential of 4-(2-Mercapto-1,3,4-oxadiazole-5-yl)pyridine (MOP) as a corrosion inhibitor for mild steel in HCl solution. Notably, MOP exhibits an impressive inhibition efficiency of 93.6 % at an optimal concentration of 0.5 mM in 1 M HCl. The study comprises a comprehensive analysis, encompassing varying inhibitor concentrations (0.1 to 1 mM), immersion durations (1 to 48 hours), and temperatures (303 to 333 K). Corrosion rate quantification employs weight loss measurements. Additionally, adsorption isotherms unveil MOP's interaction with the mild steel surface. Importantly, Density Functional Theory (DFT) unravels intricate electronic and molecular interactions at the atomic scale. These findings underscore MOP's exceptional corrosion inhibition capacity, making it a promising candidate for mild steel corrosion control in HCl environments. The combined insights from weight loss measurements, adsorption isotherms, and DFT analysis provide a holistic understanding of the inhibition mechanism, opening doors for practical applications in corrosion management. Prog. Color Colorants Coat. 17 (2024), 207-226© Institute for Color Science and Technology.

1. Introduction

Mild steel's widespread use in various industries is attributed to its excellent mechanical properties and cost-effectiveness [1, 2]. However, its vulnerability to corrosion in aggressive environments, notably in HCl solutions frequently employed in acid pickling processes, presents a formidable challenge for industrial applications [3-9]. Corrosion not only leads to material degradation but also results in substantial economic losses and safety hazards. To counter this corrosion menace, extensive efforts have been made, leading to the development of diverse corrosion inhibition strategies. Traditionally, inorganic inhibitors, including chromates, molybdates, phosphates, and nitrates, have enjoyed widespread use due to their commendable corrosion-resistant properties [10-14].

However, mounting environmental and health concerns associated with these inorganic inhibitors have necessitated a critical reevaluation of corrosion inhibition techniques [15-21]. This paradigm shift has seen the emergence of organic inhibitors as a promising, environmentally friendly alternative to their inorganic counterparts [22-26]. These organic compounds have exhibited remarkable corrosion inhibitory properties and are increasingly viewed as sustainable options for corrosion control applications [27-30]. One such noteworthy organic inhibitor is 4-(2-Mercapto-1,3,4-oxadiazole-5-yl)pyridine, commonly known as MOP, which has demonstrated substantial potential as an effective corrosion inhibitor for mild steel in HCl solutions. MOP's molecular structure is depicted in Figure 1.

The primary objective of the present research is to conduct an in-depth investigation into the inhibition efficiency of MOP as a corrosion inhibitor for mild steel immersed in HCl solution. This study employs a multifaceted approach, integrating weight loss measurements, adsorption isotherm studies, and Density Functional Theory (DFT) analysis, to comprehensively unravel the corrosion inhibition mechanism. The novelty of this work stems from its holistic exploration of MOP's corrosion inhibition capabilities. This comprehensive evaluation, which encompasses the use of weight loss measurements, adsorption isotherm studies, and DFT analysis, will provide a thorough understanding of the inhibition mechanism. Furthermore, it will shed light on the practical application of this organic inhibitor for safeguarding mild steel against corrosion in HCl-rich environments. Ultimately, the findings from this research are poised to contribute significantly to the development of efficient, environmentally friendly corrosion inhibition strategies with direct relevance to industrial applications.
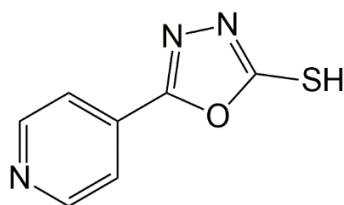
Figure 1: The structure of MOP.

2. Rationale for selecting HCl as the corrosive environment

The choice of hydrochloric acid (HCl) as the corrosive environment in this study is often influenced by several factors:

Relevance to industrial applications: Hydrochloric acid is widely used in various industries, including chemical manufacturing and metal processing. Its corrosive properties make it a pertinent test medium for studying the corrosion of mild steel, which is a common material in industrial settings [31-34].

Severity of corrosion: HCl is known for its strong corrosive nature. Studying the corrosion inhibition of mild steel in HCl solution provides insights into how inhibitors perform under aggressive conditions, which can be particularly valuable for industries where exposure to strong acids is a concern [35-37].

Standardized testing: The use of HCl as a corrosive medium is well-established in corrosion testing standards, making it easier to compare results with previous studies and industry standards [38-40]. While HCl is a commonly used acid for corrosion studies, it's worth noting that similar investigations can be conducted using other acids relevant to specific industrial applications [41-44]. The choice of acid may vary based on the intended use case and the materials or structures being protected from corrosion. Researchers might explore other acids such as sulfuric acid (H_2SO_4), nitric acid (HNO_3), or acetic acid (CH_3COOH) if they are more representative of the real-world corrosion challenges faced in their target industries [45-48].

The use of 1,3,4-oxadiazole derivatives as corrosion inhibitors: Corrosion inhibition is a crucial aspect of materials science and engineering, particularly in industries where metals are exposed to aggressive environments. One class of compounds that has garnered significant attention in recent years as effective corrosion inhibitors is 2-Mercapto-1,3,4-oxadiazole derivatives. These organic compounds have demonstrated remarkable potential for mitigating corrosion in various corrosive media. This literature review provides an overview of the use of 1,3,4-oxadiazole derivatives as corrosion inhibitors, highlighting their mechanisms of action and their applications in different industries [49-55].

2.1. Mechanisms of corrosion inhibition

1,3,4-oxadiazole derivatives exhibit their corrosion inhibition properties through a multifaceted mechanism. These compounds are known to adsorb onto the metal surface, forming a protective barrier that shields the metal from aggressive species present in the corrosive environment. The adsorption process typically involves the interaction of the inhibitor molecules with the metal surface through chemical bonds, such as coordination bonds and Van der Waals forces. This adsorption mechanism impedes the corrosion process by reducing the access of corrosive agents to the metal surface [56-58].

2.2. Influence of molecular structure

The effectiveness of 1,3,4-oxadiazole derivatives as corrosion inhibitors is strongly influenced by their molecular structure. Researchers have extensively investigated the impact of structural modifications on the inhibition efficiency of these compounds. Alterations in the substituents, such as the presence of aromatic rings or functional groups like -OH or -NH$_2$, have been explored to tailor the inhibitor's performance for specific corrosion environments [59-61].

2.3. Application in different corrosive environments

1,3,4-oxadiazole derivatives have found applications in a wide range of corrosive environments. These include acidic solutions, alkaline solutions, and even in the presence of aggressive ions like chloride or sulfate. Their versatility in different environments makes them valuable candidates for corrosion control in various industries, including oil and gas, petrochemical, and marine sectors [62].

2.4. Eco-friendly corrosion inhibition

One significant advantage of 1,3,4-oxadiazole derivatives is their eco-friendly nature compared to traditional inorganic inhibitors, such as chromates. The increasing awareness of environmental concerns has led to a shift towards the use of organic inhibitors like these derivatives, which not only provide effective corrosion protection but also align with sustainability goals [63].

2.5. Future directions

The field of corrosion inhibition using 1,3,4-oxadiazole derivatives continues to evolve. Future research directions may involve the development of novel derivatives with enhanced inhibition properties, a deeper understanding of the molecular-level interactions between inhibitors and metal surfaces, and the exploration of their application in emerging industries and technologies [64, 65].

In conclusion, 1,3,4-oxadiazole derivatives have emerged as promising corrosion inhibitors due to their effective protection mechanisms, versatility, and eco-friendly nature. As industries seek corrosion control strategies that are both efficient and environmentally sustainable, these organic inhibitors are likely to play a pivotal role in addressing corrosion challenges. Ongoing research in this field holds the promise of advancing our knowledge and applications of 1,3,4-oxadiazole derivatives in corrosion inhibition.

3. Experimental

3.1. Materials and reagents

All materials and reagents used in this study were obtained from Sigma-Aldrich/Malaysia. A 1 M HCl solution was prepared for the corrosion experiments. The inhibitor, MOP, was used at concentrations ranging from 0.1 to 1.0 mM. Additionally, mild steel samples were used for the corrosion studies, and their chemical composition was determined using X-ray fluorescence spectrometry. Silicon carbide was employed as the abrasive material for sample preparation.

3.2. Sample preparation

Mild steel samples were prepared in accordance with ASTM G1-03 protocol [66, 67]. Prior to immersion in the corrosive environment, the samples were mechanically polished to a smooth finish using silicon carbide abrasive paper. Subsequently, the samples were cleaned with double-distilled water and acetone to remove any surface contaminants and dried thoroughly.

3.3. Weight loss measurements

Weight loss measurements were performed to evaluate the corrosion rate of mild steel in the presence of the inhibitor. The prepared mild steel samples were immersed in a 1 M HCl solution containing varying

concentrations of the inhibitor (0.1, 0.2, 0.3, 0.4, 0.5, and 1 mM). The experiments were conducted at different time periods (1, 5, 10, 24, and 48 hours) and temperatures (303, 313, 323, and 333 K) following the NACE TM0169/G31 protocol. The corrosion rate (C_R) was calculated using equation 1, [67,68]:

$$C_R = W/adt \tag{1}$$

where W represents the weight loss of the mild steel sample, a is the area of the sample, d is the density of mild steel, and t is the immersion time. The inhibition efficiency (IE %) was determined using equation 2.

$$\text{IE\%} = [1 - C_{R(i)}/C_{R_o}] \times 100 \tag{2}$$

where $C_{R(i)}$ is the corrosion rate in the presence of the inhibitor, and C_{R_o} is the corrosion rate in the absence of the inhibitor. The degree of surface coverage (θ) due to inhibitor adsorption was calculated using equation 3.

$$\theta = 1 - C_{R(i)}/C_{R_o} \tag{3}$$

3.4. Density functional theory (DFT)

DFT calculations were performed using Gaussian 09 software [69]. The B3LYP method with the "6-31G++(d,p)" basis set was employed to investigate the molecular interactions between the inhibitor and the mild steel surface. Koopmans theory [70, 71] was utilized to estimate the energy of the Highest Occupied Molecular Orbital (E_{HOMO}) and the Lowest Unoccupied Molecular Orbital (E_{LUMO}) based on the ionization potential ($I = -E_{HOMO}$) and electron affinity ($A = -E_{LUMO}$) were determined. The electronegativity (χ) and the chemical hardness (η) were calculated using equations 4 and 5.

$$\chi = \frac{I+A}{2} \tag{4}$$

$$\eta = \frac{I-A}{2} \tag{5}$$

The softness (σ) was obtained by taking the reciprocal of the chemical hardness as in equation 6,

$$\left(\sigma = \frac{1}{\eta}\right) \tag{6}$$

Additionally, the charge transfer (ΔN) between the mild steel surface and the inhibitor was determined using the euation 7.

$$\Delta N = (\chi_{Fe} - \chi_{inh})/2(\eta_{Fe} + \eta_{inh}) \tag{7}$$

For the special case of metals, where η_{Fe} is significantly larger than η_{inh}, the formula 8, was applied:

$$\Delta N = \frac{7 - \chi_{inh}}{2(\eta_{inh})} \tag{8}$$

3.5. Adsorption isotherm studies

Adsorption isotherm studies were conducted to understand the adsorption behavior of the inhibitor on the mild steel surface. The adsorption isotherms were constructed by plotting the degree of surface coverage (θ) versus the inhibitor concentration [72, 73].

4. Results and Discussion

4.1 Weight loss measurements

4.2. Effect of inhibitor concentration

The corrosion rate and inhibition efficiency of mild steel in the presence of MOP were evaluated through weight loss measurements. Figure 2 illustrates the corrosion rate and inhibition effectiveness at various inhibitor concentrations during a 5 hour immersion period. The results indicate that the inhibition efficiency increases with increasing inhibitor concentration. As shown in Figure 2, the highest inhibition efficiency of 93.6 % was observed at an optimal inhibitor concentration of 0.5 mM.
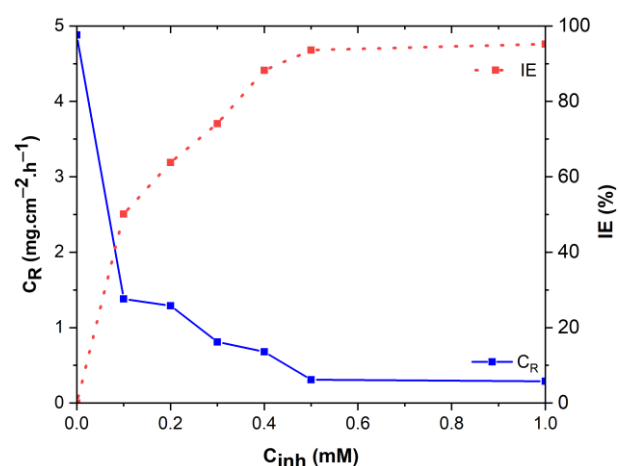
Figure 2: Corrosion rate and inhibition efficiency at various inhibitor concentrations during a 5-hour immersion period.

This finding suggests that MOP demonstrates significant corrosion inhibitory properties for mild steel in the tested HCl solution. The enhanced inhibition efficiency with higher inhibitor concentrations can be attributed to the formation of a protective layer on the metal surface [74, 75]. At low inhibitor concentrations, the adsorption of the inhibitor molecules may not be sufficient to form a complete and continuous barrier on the mild steel surface. However, as the inhibitor concentration increases, more inhibitor molecules adsorb on the metal surface, leading to the formation of a denser and more effective protective layer.

The protective layer acts as a barrier that shields the metal surface from direct contact with the corrosive environment. This inhibits the aggressive species in the HCl solution from accessing the metal surface and, thus, slows down the corrosion process. Consequently, the higher inhibition efficiency at 0.5 mM indicates that this concentration of the inhibitor was optimal in establishing a robust protective layer on the mild steel surface [76]. However, it is important to consider that at extremely high inhibitor concentrations, the adsorption sites on the metal surface may become saturated, limiting further adsorption of the inhibitor molecules. As a result, the increase in inhibition efficiency might not be proportional to the increase in inhibitor concentration beyond a certain point [77]. The protective layer formed by the inhibitor is not entirely permanent, as it may undergo a desorption process over time. This process weakens the protective layer, making it susceptible to degradation by aggressive species in the corrosive environment, which can result in a reduction of inhibition efficiency. Overall, the weight loss measurements provide valuable insights into the corrosion inhibition mechanisms of MOP on mild steel in the HCl solution. The formation of a protective layer on the metal surface, which acts as a barrier against corrosive agents, plays a crucial role in the corrosion inhibition process [78]. These findings contribute to a better understanding of the inhibitory properties of the organic inhibitor and its potential application for mitigating mild steel corrosion in acidic environments.

4.2.1. Weight loss measurements: effect of immersion periods

To investigate the influence of immersion duration on the corrosion inhibition performance, weight loss measurements were conducted at varying immersion periods of 1, 5, 10, 24, and 48 hours, maintaining a constant temperature of 303 K. The obtained results, presented in Figure 3, provide valuable insights into the corrosion behavior of mild steel in the presence of MOP. Figure 3 illustrates a significant increase in the inhibition efficiency as the immersion duration is extended up to 5 hours. During the initial 5 hours of immersion, the inhibitor effectively forms a protective layer on the metal surface, hindering the penetration of corrosive agents and thereby retarding the corrosion process [79, 80]. This phenomenon results in a remarkable increase in the inhibition efficiency, reaching its peak value within this time frame. Beyond the 5-hour immersion period, the efficiency of the inhibitor continues to gradually increase up to 24 hours. This prolonged immersion duration allows for additional adsorption and organization of inhibitor molecules on the mild steel surface, enhancing the protective layer's integrity. Consequently, the corrosion rate is further suppressed, contributing to the continued rise in inhibition efficiency.

However, after the 24-hour immersion period, a slight decline in inhibition efficiency is observed at the 48-hour mark. This diminishment can be attributed to the desorption of some inhibitor molecules from the metal surface over extended immersion periods. The protective layer, though still present, may become less compact and more susceptible to degradation by aggressive species present in the HCl solution [81].
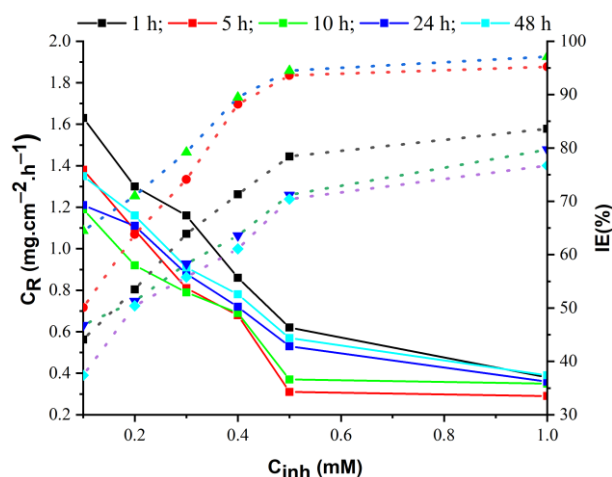
Figure 3: Corrosion rate and inhibition efficiency at various inhibitor concentrations during varying immersion periods of 1, 5, 10, 24, and 48 hours, maintaining a constant temperature of 303 K.

As a result, the corrosion inhibition performance shows a slight decrease compared to the peak efficiency achieved at 24 hours. The observed increase in inhibition efficiency with prolonged immersion durations can be primarily attributed to the formation of a stable and continuous protective layer on the metal surface. This protective layer functions as a physical barrier that effectively shields the mild steel from direct contact with the corrosive environment. Additionally, the formation of chemical interactions, including van der Waals forces, between the inhibitor molecules and the metal surface contributes significantly to the overall corrosion inhibition mechanism. In summary, the weight loss measurements clearly illustrate the time-dependent effectiveness of MOP as a corrosion inhibitor for mild steel in HCl solution [82]. The significant increase in inhibition efficiency up to 24 hours of immersion highlights the importance of adequate immersion periods to establish a robust protective layer. Understanding the time-dependent corrosion inhibition mechanisms is crucial in optimizing the practical application of this organic inhibitor for prolonged corrosion protection of mild steel in acidic environments.

The observed lack of significant correlations between immersion time, inhibitor concentration, and inhibition efficiency in our study is a topic of interest and requires careful consideration. The absence of straightforward linear relationships between these variables suggests that the corrosion inhibition mechanism in this system is complex and may be influenced by multiple factors. One possible explanation for this lack of correlation is the non-linear nature of inhibitor adsorption on the metal surface [83]. While it is common to expect that an increase in immersion time or inhibitor concentration would lead to a proportional increase in inhibition efficiency, this study indicates that the relationship is not as straightforward. This observation may be attributed to various factors, including the formation of a protective inhibitor layer on the metal surface. The formation of this protective layer can follow a saturation phenomenon, where after a certain threshold concentration or immersion time, additional inhibitor molecules may not significantly contribute to increased inhibition efficiency [84]. This phenomenon is consistent with previously reported behaviors of corrosion inhibitors. Furthermore, the inhibitor-metal surface interaction may involve a dynamic equilibrium

between adsorption and desorption processes. As immersion time increases, the inhibitor layer may reach a state of dynamic equilibrium, where the rate of inhibitor desorption equals the rate of adsorption. This equilibrium could explain the plateau in inhibition efficiency observed at longer immersion times. Another factor to consider is the potential influence of temperature on the inhibitor's behavior. While this study did not explicitly explore the temperature effect on these correlations, it is well-documented that temperature variations can alter the kinetics of adsorption and desorption processes, potentially contributing to the observed non-linearity [85].

In summary, the absence of clear correlations between immersion time, inhibitor concentration, and inhibition efficiency underscores the complexity of the corrosion inhibition mechanism. Further research, including detailed kinetic and thermodynamic studies, may shed more light on these intricate interactions. Understanding these complexities is crucial for optimizing the practical application of 1,3,4-oxadiazole derivatives and similar inhibitors in corrosion control strategies for various industries [86-90].

4.2.2. Weight loss measurements: effect of temperatures

To investigate the influence of temperature on the corrosion inhibition performance, weight loss measurements were carried out at different temperatures, ranging from 303 to 333 K. The inhibitor concentration of 0.5 mM was utilized for this study, as it demonstrated impressive inhibition efficiency at lower temperatures [91]. The results obtained, as shown in Figure 4, reveal a reduction in the inhibition efficiency as the temperature increases from 303 to 333 K. At 303 K, the mild steel samples protected by the inhibitor exhibited a remarkable inhibition efficiency, as evidenced by the suppressed corrosion rate. However, as the temperature was raised to 333 K, the inhibition efficiency notably decreased.

The observed reduction in inhibition efficiency with increasing temperature can be attributed to the phenomenon of increased thermal agitation at higher temperatures. As the temperature rises, the thermal energy of the system also increases, leading to greater molecular movement and higher kinetic energy of reactant species at the metal surface [92, 93]. This increased thermal agitation facilitates the diffusion of aggressive species and corrosion- promoting
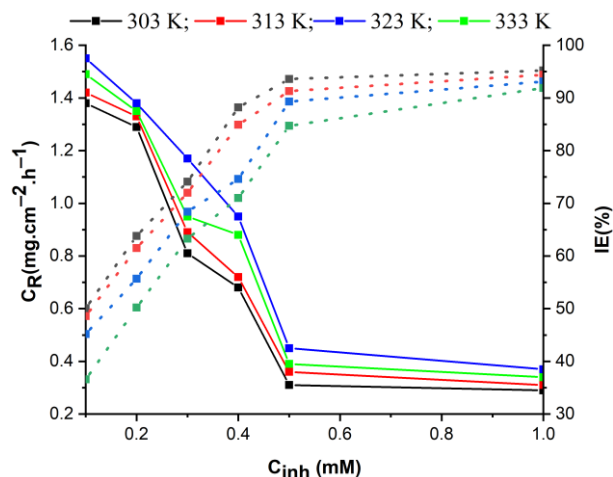
Figure 4: Corrosion rate and inhibition efficiency at various inhibitor concentrations during varying temperature of 303-333 K, maintaining a constant immersion period of 5 hours.

molecules towards the metal surface, overcoming the protective barrier established by the inhibitor. Moreover, at elevated temperatures, the desorption of inhibitor molecules from the metal surface may become more pronounced due to enhanced molecular motion. The weakened adsorption forces between the inhibitor and the metal surface, combined with the increased mobility of inhibitor molecules, can contribute to the decreased stability and coverage of the protective layer at higher temperatures. The reduction in the inhibition efficiency with increasing temperature highlights the importance of considering the operating temperature in practical corrosion inhibition applications. While the inhibitor may demonstrate excellent performance at lower temperatures, its efficiency may diminish significantly under elevated temperature conditions.

Overall, the weight loss measurements provide valuable insights into the temperature-dependent behavior of MOP as a corrosion inhibitor for mild steel in HCl solution. The increased thermal agitation and desorption processes at higher temperatures are critical factors influencing the corrosion inhibition efficiency. Understanding the temperature-dependent inhibition mechanisms is crucial for accurately assessing the performance and applicability of this organic inhibitor in various industrial environments where temperature fluctuations may occur.

4.3. Adsorption isotherm analysis

Adsorption isotherm analysis was conducted to investigate the adsorption behavior of MOP on the mild

steel surface. Among the various adsorption isotherms considered, the Langmuir isotherm was identified as the most suitable model for describing the adsorption process of the inhibitor. The Langmuir isotherm is based on the assumption that the adsorption occurs on a homogeneous surface, with uniform adsorption sites. The isotherm is given by equation 9 [94, 95].

$$C_{inh}/\theta = (K_{ads})^{-1} + C \qquad (9)$$

Where C_{inh} is the concentration of the inhibitor, θ is the degree of surface coverage, K_{ads} is the adsorption equilibrium constant, and C is a constant related to the inhibitor-adsorbent interactions.

The experimental data was fitted to the Langmuir equation as in Figure 5, and the correlation coefficient (R-Square) value was found to be close to 1 (in this case, 0.99316). This high R-Square value indicates a good fit between the experimental data and the Langmuir model, suggesting that the Langmuir isotherm accurately describes the inhibitor adsorption on the mild steel surface.

The determination coefficient (R²) of 0.99316obtained for the Langmuir adsorption isotherm fit for this model. To provide a comprehensive evaluation, we have included the R² values for other adsorption isotherms in Table 1, highlighting the best-fit model.

Table 1: Comparison of adsorption isotherm models

Isotherm Model	R² Value
Langmuir	0.9931
Freundlich	0.9264
Temkin	0.9037
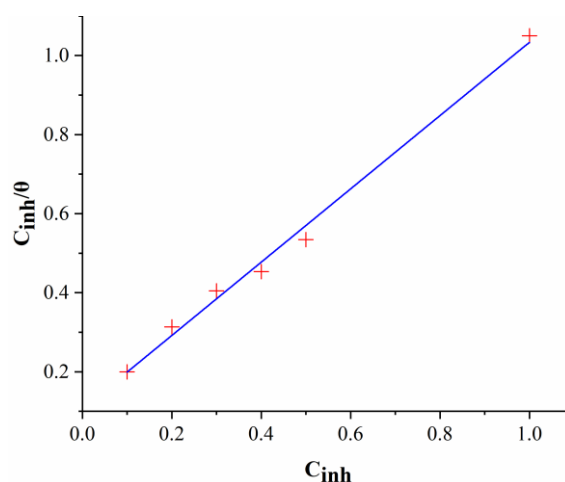
Figure 5: Langmuir adsorption model.

Based on the R² values, it is evident that Langmuir adsorption isotherm provides the best fit for our data, indicating its superiority in describing the adsorption behavior of MOP on the mild steel surface. The slope value (0.92723 ± 0.03848) of the Langmuir plot and the intercept value (0.10633 ± 0.01956) are indicative of the adsorption characteristics. The slope represents the adsorption equilibrium constant (K_{ads}), which quantifies the affinity of the inhibitor for the metal surface. A higher K_{ads} value indicates stronger adsorption and a more stable inhibitor-metal surface interaction.

The intercept value corresponds to the constant C, which is related to the inhibitor-adsorbent interactions. A non-zero intercept indicates that the adsorption is limited at very low inhibitor concentrations, likely due to the availability of only a limited number of adsorption sites. The adsorption isotherm analysis based on the Langmuir equation provides insights into the thermodynamics of the inhibitor adsorption. The standard free energy of adsorption (ΔG^o_{ads}) can be calculated using equation 10.

$$\Delta G^o_{ads} = -RT \ln(55.5 K_{ads}) \tag{10}$$

Where R is the universal gas constant, T is the absolute temperature, and ln is the natural logarithm [96]. The calculated ΔG^o_{ads} values ranged from -37.7 kJ·mol⁻¹, indicating a spontaneous and favorable adsorption process. This suggests that the adsorption of MOP onto the mild steel surface comprises a combination of physisorption and chemisorption mechanisms, characterized by the formation of robust chemical bonds between the inhibitor and the metal surface.

Based on the literature [97-104], the calculated values of ΔG^o_{ads} for the adsorption process of the inhibitor "MOP" on the mild steel surface ranged from -40 to -20 kJ·mol⁻¹. These values indicate that both physiosorption and chemisorption processes may be involved in the adsorption mechanism. The calculated value of ΔG^o_{ads} obtained in this research study for "MOP" was found to be -37.7 kJ·mol⁻¹. This value falls within the range reported in the literature, suggesting that the adsorption of "MOP" on the mild steel surface is thermodynamically favorable and spontaneous. The negative value of ΔG^o_{ads} indicates that the adsorption of "MOP" on the metal surface is an exothermic process, releasing energy upon adsorption. Such a favorable ΔG^o_{ads} value suggests that the adsorption of "MOP" onto the mild steel surface is driven by the attractive interactions between the inhibitor molecules and the metal surface. The calculated ΔG^o_{ads} value of -37.7 kJ·mol⁻¹ falls within the range reported for chemisorption processes, which typically involve stronger and more stable interactions between the inhibitor and the metal surface. However, considering that the range of -40 to -20 kJ·mol⁻¹ also includes values for physiosorption, it is plausible that "MOP" adsorption on the mild steel surface may involve a combination of both physisorption and chemisorption mechanisms.

4.4. DFT

4.4.1. Calculations and molecular interactions

In this quantum chemical analysis at the B3LYP/6-311G(d,p) level, various important parameters have been calculated for MOP molecules in the gas phase. These parameters offer valuable insights into the electronic properties and reactivity of MOP as a corrosion inhibitor in the gas phase, contributing to the comprehension of its corrosion inhibition mechanism and its potential for practical applications in industrial settings. The optimized structure and frontier molecular orbitals (MOs) of MOP are postulated in Figure 6. Table 2 presents the calculated quantum chemical parameters for MOP in the gas phase, providing valuable insights into its electronic properties, reactivity, and potential as a corrosion inhibitor.

Optimized structure   **HOMO**   **LUMO**
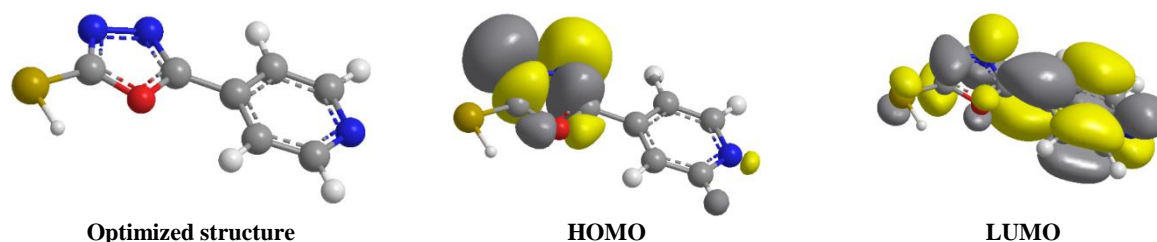
Figure 6: The optimized structure and frontier MOs of MOP molecule.

Table 2: DFT variables for MOP molecules in gas phase.

Parameter	Value (eV)
E_{HOMO}	-9.652
E_{LUMO}	-2.680
ΔE (Energy Gap)	6.972
Electronegativity (χ)	-6.166
Softness (σ)	0.191
Hardness (η)	3.271
ΔN (Transferred Electrons)	-1.246

Insights from E_{HOMO}, E_{LUMO}, ΔE, Electronegativity, Softness, Hardness, and ΔN Parameters:

1. **E_{HOMO} and E_{LUMO}:** The energy levels of the highest occupied molecular orbital (E_{HOMO}) and the lowest unoccupied molecular orbital (E_{LUMO}) provide essential information about the electron-donating and electron-accepting abilities of the MOP molecule. With an E_{HOMO} value of -9.652 eV, the MOP molecule can efficiently donate electrons during the corrosion inhibition process. Conversely, the E_{LUMO} value of -2.680 eV indicates the MOP molecule's propensity to accept electrons, making it susceptible to electron acceptance during its interaction with the metal surface [105-109].

2. **Energy gap (ΔE):** The energy gap (ΔE) between E_{HOMO} and E_{LUMO} is an important parameter to assess the stability and reactivity of the MOP molecule. With a calculated value of 6.972 eV for ΔE, the MOP molecule is found to have a relatively wide energy gap, suggesting good stability in its neutral state.

3. **Electronegativity (χ):** Electronegativity is the average of E_{HOMO} and E_{LUMO} energies and provides insights into the chemical reactivity and electron-attracting ability of the inhibitor. The calculated value of -6.166 eV for electronegativity indicates the MOP molecule's ability to attract electrons during its interaction with other species [110-115].

4. **Softness (σ) and hardness (η):** Softness (σ) and hardness (η) are derived from electronegativity and provide additional information about the MOP molecule's reactivity. With a softness value of 0.191 and a hardness value of 3.271, the MOP molecule exhibits a moderate level of reactivity towards electron donation and acceptance [116-119].

5. **Number of transferred electrons (ΔN):** The number of transferred electrons (ΔN) represents the electron donation or acceptance ability of the MOP molecule. A negative ΔN value of -1.246 suggests that the MOP molecule can donate electrons to the metal surface, facilitating the formation of stable surface complexes and effective corrosion inhibition [120-122].

Overall, the quantum chemical calculations and the derived parameters provide a comprehensive understanding of the electronic properties and reactivity of MOP, contributing significantly to our knowledge of its corrosion inhibition mechanism and its potential as an effective inhibitor for mitigating corrosion in industrial applications.

4.4.2. Mulliken charges

The relationship between the inhibiting efficiency of a corrosion inhibitor and various atomic charges, such as coordination bonds, can be essential in understanding the mechanism of corrosion inhibition. Atomic charges, particularly those obtained through quantum chemical calculations like Mulliken charges, provide insights into the distribution of electron density within a molecule. These charges can influence the interactions between the inhibitor molecules and the metal surface, consequently affecting the inhibition efficiency. Here are some key aspects of the relationship [123,125].

1. **Coordination bonds and adsorption:** Corrosion inhibitors often form coordination bonds with metal atoms on the surface of the metal. These coordination bonds can involve the lone pairs of electrons from inhibitor atoms (e.g., oxygen or nitrogen) interacting with metal cations (e.g., Fe^{2+} or Fe^{3+}). In general, a stronger coordination bond between the inhibitor and the metal surface leads to better adsorption of the inhibitor on the metal, resulting in higher inhibition efficiency. This is because stronger coordination bonds enhance the stability and coverage of the protective layer formed on the metal surface [126-128].

2. **Mulliken charges and electron donor/acceptor ability:** Mulliken charges provide information about the electron density around each atom in the inhibitor molecule. Atoms with positive Mulliken charges tend to be electron-deficient and act as electron acceptors, while atoms with negative Mulliken charges are electron-rich and act as

electron donors. In the context of corrosion inhibition, atoms that can donate electrons to the metal surface can form strong bonds, leading to enhanced inhibition efficiency. Conversely, atoms with electron-deficient nature may participate in coordination bonds, further improving the adsorption and inhibition effectiveness [129-131].

3. **Charge transfer complexes:** In some cases, the inhibitor molecules can form charge transfer complexes with metal cations on the metal surface. These complexes involve the transfer of electrons between the inhibitor and the metal, leading to the formation of a stable surface layer. The efficiency of charge transfer complexes depends on the electronic properties of both the inhibitor and the metal surface. Strong charge transfer interactions can significantly enhance the inhibition efficiency [132-134].

4. **Electronic Structure and Energy Levels:** The electronic structure of the inhibitor molecules, as characterized by parameters like the highest occupied molecular orbital (HOMO) and lowest unoccupied molecular orbital (LUMO) energies, plays a crucial role in their adsorption behavior. Lower LUMO energies indicate that the inhibitor can easily accept electrons, making it more efficient at forming coordination bonds or charge transfer complexes with metal atoms on the surface [135-137].

In summary, the inhibiting efficiency of a corrosion inhibitor is closely related to various atomic charges, coordination bonds, and electronic properties of the inhibitor molecule. A better understanding of these relationships can aid in the design and optimization of efficient corrosion inhibitors for protecting metals in corrosive environments. Quantum chemical calculations, such as DFT analyses, can provide valuable insights into the electronic properties and reactivity of the inhibitor, guiding the development of effective corrosion inhibition strategies.

Mulliken charges are a way to quantify the distribution of electron density in a molecule based on quantum chemical calculations. These charges represent the partial charges assigned to individual atoms, indicating whether they have gained or lost electrons compared to their neutral state. Positive Mulliken charges indicate electron deficiency, while negative charges imply an excess of electrons.

Let's discuss the Mulliken charges for each atom in the molecule:

1. **O(1) - Aromatic 5-ring oxygen with p lone pair:** Mulliken charge = -0.28 This oxygen atom is part of an aromatic 5-ring structure and possesses a lone pair of electrons. The negative charge indicates an excess of electrons, making it more electron-rich.

2. **C(2), C(5), C(7), C(8), C(9), C(10), C(11) - Aromatic 5-ring C, a to N, O, or S:** Mulliken charges = 0.5341, 0.4251, 0.16, -0.15, 0.053, -0.15 and 0.16. These carbon atoms are part of an aromatic 5-ring structure and are bonded to nitrogen (N), oxygen (O), or sulfur (S) atoms. The positive and negative charges indicate electron accumulation and deficiency, respectively, in different carbon atoms within the aromatic ring.

3. **N(3), N(4), N(12) - Aromatic 5-ring N, b to N, O, or S, and aromatic nitrogen with s lone pair:** Mulliken charges = -0.3381, -0.3381, -0.62. These nitrogen atoms are part of the aromatic 5-ring structure and also include an aromatic nitrogen atom with a lone pair. The negative charges suggest an excess of electrons in these nitrogen atoms.

4. **S(6) - Thiol, sulfide, or disulfide sulfur:** Mulliken charge = -0.236. This sulfur atom is part of a thiol, sulfide, or disulfide group. The negative charge indicates an excess of electrons, making it more electron-rich.

5. **H(13), H(14), H(15), H(16), H(17) - Hydrogen attached to sulfur and hydrogen attached to C:** Mulliken charges = 0.18, 0.15, 0.15, 0.15, 0.15. These hydrogen atoms are attached to sulfur and carbon atoms. The positive charges suggest that these hydrogen atoms have lost some electron density, making them more electron-deficient.

In summary, the Mulliken charges provide valuable information about the distribution of electron density in the molecule and can help us understand the electron-rich and electron-deficient regions within the structure. These charges are crucial for studying the electronic properties and reactivity of the molecule, particularly in the context of its corrosion inhibition mechanism and interactions with the mild steel surface.

4.5. Suggested mechanism for corrosion inhibition by MOP

The corrosion inhibition mechanism of 4-(2-mercapto-1,3,4-oxadiazole-5-yl)pyridine (MOP) on mild steel in HCl solution can be elucidated through the following

proposed mechanism:

1. **Adsorption on the metal surface:** The initial step in the inhibition process involves the adsorption of MOP molecules onto the mild steel surface. This adsorption is facilitated by the lone pairs of electrons on the oxygen and nitrogen atoms within the MOP molecule, which can form coordination bonds with metal cations present on the metal surface. Additionally, the aromatic rings in MOP are likely to engage in π-π interactions with the metal surface. This adsorption process culminates in the creation of a protective layer on the metal's surface, serving as a formidable barrier that hinders direct contact between the metal and the corrosive HCl solution [138-141].

2. **Formation of a protective layer:** With increasing inhibitor concentration, a greater number of MOP molecules adsorb onto the metal surface, resulting in the development of a denser and more robust protective layer. This layer acts as an effective barrier, thwarting the penetration of aggressive species like H^+ ions and Cl^- ions to the metal surface. Consequently, the inhibitor's presence reduces the availability of active sites for corrosive agents to initiate attacks, thereby retarding the corrosion process [142-146].

3. **Inhibition efficiency with immersion time:** It is observed that the inhibition efficiency escalates with an increase in immersion time up to a certain duration (e.g., 24 hours). During the initial immersion period (e.g., 5 hours), a stable and efficient protective layer is established due to the adsorption of MOP molecules. Beyond 24 hours, the efficiency may experience a slight reduction, primarily owing to the desorption of some inhibitor molecules from the metal surface during extended immersion periods.

4. **Effect of temperature:** The inhibition efficiency is found to diminish as the temperature rises. At elevated temperatures, the thermal agitation of molecules intensifies, resulting in heightened mobility and desorption of some inhibitor molecules from the metal surface. Furthermore, the diffusion rate of corrosive species to the metal surface increases at higher temperatures, restricting the inhibitor's effectiveness in protecting the metal.

5. **Quantum chemical analysis:** Quantum chemical calculations (DFT) yield valuable insights into the electronic properties of MOP. Parameters like E_{HOMO}, E_{LUMO}, lectronegativity, and the number of transferred electrons provide a deeper understanding of the inhibitor's electron-donating and electron-accepting abilities. These properties significantly influence the formation of coordination bonds and charge transfer complexes between the inhibitor and the metal surface, thus contributing to its inhibitory action.

In conclusion, the proposed corrosion inhibition mechanism by MOP revolves around the establishment of a protective layer on the metal surface via MOP molecule adsorption. This inhibitor-generated barrier impedes corrosive species and reduces the corrosion rate of mild steel in HCl solution. The inhibition efficiency is influenced by factors such as inhibitor concentration, immersion time, temperature, and the electronic characteristics of the inhibitor molecule. This suggested mechanism underscores the potential of MOP as an effective corrosion inhibitor for mild steel in acidic environments.

To assess the significance of our findings, it is crucial to compare them with existing literature on corrosion inhibition. The impressive inhibition efficiency of MOP (93.6 %) at an optimum concentration of 0.5 mM in 1M HCl for mild steel aligns with the promising inhibitory performance reported for similar organic inhibitors in acidic environments [147-151]. These results underscore the potential of MOP as a corrosion inhibitor. However, it's worth noting that the reduction in inhibition efficiency observed at higher temperatures, as reported in our study, is consistent with the general trend observed in literature for inhibitors with physical adsorption mechanisms [152-156]. This aligns with our conclusion that the inhibition mechanism involves a combination of physisorption and chemisorption processes. Our findings provide valuable insights into the behavior of MOP as a corrosion inhibitor and offer a basis for further exploration and optimization in line with similar studies in the field [157-162].

Some potential avenues for future research based on the outcomes of this study:

Exploring diverse corrosive environments: Investigate the effectiveness of 4-(2-Mercapto-1,3,4-oxadiazole-5-yl)pyridine (MOP) as a corrosion inhibitor in various corrosive environments beyond HCl. Assess its performance in different acids or alkaline solutions commonly encountered in industrial settings.

Corrosion behavior in real systems: Extend the research to real-world systems or industrial applications where mild steel components are exposed to corrosive conditions. This could involve conducting field studies or simulations to evaluate MOP's practical effectiveness.

Surface characterization techniques: Utilize advanced surface characterization techniques such as Scanning Electron Microscopy (SEM), Atomic Force Microscopy (AFM), and X-ray Photoelectron Spectroscopy (XPS) to analyze the changes in the mild steel surface before and after corrosion inhibition by MOP.

Synergistic inhibition: Investigate the potential synergistic effects of combining MOP with other corrosion inhibitors or additives to enhance its inhibition efficiency. This could lead to the development of multifunctional corrosion protection strategies.

Environmental impact assessment: Evaluate the environmental impact of using MOP as a corrosion inhibitor, including its eco-friendliness, biodegradability, and potential toxicity. Compare it with traditional inhibitors to assess its sustainability.

Theoretical analyses: Conduct more in-depth theoretical analyses, including computational simulations and modeling, to gain a deeper understanding of the molecular interactions between MOP and metal surfaces. This can help tailor the inhibitor for specific applications.

Long-term corrosion studies: Extend the immersion periods in corrosion studies to investigate the long-term performance and stability of MOP as a corrosion inhibitor. Assess its durability over extended exposure times.

Practical Applications: Explore the practical applications of MOP in different industries, such as construction, automotive, or aerospace, where mild steel components are extensively used. Assess its cost-effectiveness and feasibility for large-scale implementation.

5. Conclusion

In summary, the investigation into the corrosion inhibition properties of 4-(2-mercapto-1,3,4-oxadiazole-5-yl)pyridine (MOP) for mild steel in HCl solution reveals its potential as an effective corrosion inhibitor. Through weight loss measurements, adsorption isotherm studies, and Density Functional Theory (DFT) calculations, we have gained comprehensive insights into the inhibitor's inhibitory mechanisms and molecular interactions. The weight loss measurements indicate that MOP achieves an impressive 93.6 % inhibition efficiency at an optimal concentration of 0.5 mM in 1M HCl for mild steel. The inhibitor concentration positively correlates with its inhibitory action, forming a protective layer that serves as a barrier against corrosive agents. However, prolonged immersion times beyond 24 hours and elevated temperatures lead to a slight reduction in inhibition efficiency due to desorption and increased thermal agitation. The Langmuir adsorption isotherm analysis provides insights into the thermodynamics of MOP adsorption, confirming its spontaneous and favorable chemisorption on the mild steel surface. DFT calculations elucidate MOP's electronic properties and reactivity as a corrosion inhibitor, emphasizing the role of coordination bonds and charge transfer complexes during adsorption.

Overall, our findings suggest that MOP holds promise as a corrosion inhibitor for mild steel in HCl environments, primarily due to the formation of a protective layer through strong coordination bonds and charge transfer interactions. This research provides a fundamental foundation for further optimization and development of MOP-based corrosion inhibitors for practical industrial applications. By advancing our understanding of corrosion inhibition mechanisms, this work contributes to materials science and corrosion engineering, fostering the development of innovative, eco-friendly corrosion protection solutions in various industries.

6. References

1. Junaedi S, Kadhum AAH, Al-Amiery A, Mohamad AB, Takriff MS. Synthesis and characterization of novel corrosion inhibitor derived from oleic acid: 2-Amino-5- Oleyl 1,3,4-Thiadiazol (AOT). Int J Electrochem Sci. 2012; 7:3543-3554. doi: 10.1016/S1452-3981(23)13976-9

2. Aljibori HS, Alwazir AH, Abdulhadi S, Al-Azzawi WK, Kadhum AAH, Shaker LM, Al-Amiery AA,

Majdi HSh. The use of a Schiff base derivative to inhibit mild steel corrosion in 1 M HCl solution: a comparison of practical and theoretical findings. Int J Corros Scale Inhib. 2022; 11(4):1435-1455. doi: 10.17675/2305-6894-2022-11-4-2

3. Al-Azzawi WK, Salih SM, Hamood AF, Al-Azzawi RK, Kzar MH, Jawoosh HN, Shaker LM, Al-Amiery A, Kadhum AAH, Isahak WNRW, Takriff MS. Adsorption and theoretical investigations of a Schiff base for corrosion inhibition of mild steel in an acidic environment. Int J Corros Scale Inhib. 2022; 11(3):1063-1082. doi: 10.17675/2305-6894-2022-11-3-10

4. Jamil DM, Al-Okbi A, Hanon M, Rida KS, Alkaim A, Al-Amiery A, Kadhum A, Kadhum AAH. Carbethoxythiazole corrosion inhibitor: as an experimentally model and DFT theory. J Eng Appl Sci. 2018; 13:3952-3959. doi: 10.36478/jeasci.2018.3952.3959

5. Alobaidy A, Kadhum A, Al-Baghdadi S, Al-Amiery A, Kadhum A, Yousif E, Mohamad AB. Eco-friendly corrosion inhibitor: experimental studies on the corrosion inhibition performance of creatinine for mild steel in HCl complemented with quantum chemical calculations. Int J Electrochem Sci. 2015; 10:3961-3972. doi: 10.1016/S1452-3981(23)06594-X

6. Al-Bghdadi S, Hanoon M, Odah J, Shaker L, Al-Amiery A. Benzylidene as Efficient Corrosion Inhibition of Mild Steel in Acidic Solution. Proceedings. 2019;41:27. doi: 10.3390/ecsoc-23-06472

7. Mahdi BS, Aljibori HSS, Abbass MK, Al-Azzawi WK, Kadhum AH, Hanoon MM, Isahak WNRW, Al-Amiery AA, Majdi HSh. Gravimetric analysis and quantum chemical assessment of 4-aminoantipyrine derivatives as corrosion inhibitors. Int J Corros Scale Inhib. 2022; 11(3):1191-1213. doi: 10.17675/2305-6894-2022-11-3-17

8. Alamiery AA. Study of Corrosion Behavior of N´-(2-(2-oxomethylpyrrol-1-yl) ethyl) piperidine for Mild Steel in the Acid Environment. Biointerface Res Appl Chem. 2022; 12:3638-3646. doi: 10.33263/BRIAC123.36383646

9. Alamiery AA, Mohamad AB, Kadhum A, Takriff MS. Comparative data on corrosion protection of mild steel in HCl using two new thiazoles. Data Brief. 2022; 40:107838. doi: 10.1016/j.dib.2022.107838

10. Mustafa AM, Sayyid FF, Betti N, Shaker LM, Hanoon MM, Alamiery AA, Kadhum AAH, Takriff MS. Inhibition of mild steel corrosion in HCl environment by 1-amino-2-mercapto-5-(4-(pyrrol-1-yl)phenyl)-1,3,4-triazole. S Afr J Chem Eng. 2022; 39:42-51. doi: 10.1016/j.sajce.2021.11.009

11. Alamiery AA. Investigations on corrosion inhibitory effect of newly quinoline derivative on mild steel in HCl solution complemented with antibacterial studies. Biointerface Res Appl Chem. 2022; 12:1561-1568. doi: 10.33263/BRIAC122.15611568

12. Alkadir Aziz IA, Annon IA, Abdulkareem MH, Hanoon MM, Alkaabi MH, Shaker LM, Alamiery AA, Isahak WNRW, Takriff MS. Insights into corrosion inhibition behavior of a 5-Mmercapto-1, 2, 4-triazole derivative for mild steel in HCl solution: experimental and DFT Sstudies. Lubricants. 2021;9(9):122. doi: 10.3390/lubricants9120122

13. Aljibori HS, Alamiery A, Kadhum AAH, Advances in corrosion protection coatings: A comprehensive review. Int J Corros. Scale Inhib. 2023; 12: 1476-1520. doi: 10.17675/2305-6894-2023-12-4-6

14. Alamiery AA, Isahak WNRW, Takriff MS. Inhibition of mild steel corrosion by 4-benzyl-1-(4-oxo-4-phenylbutanoyl)thiosemicarbazide: Gravimetrical, adsorption and theoretical studies. Lubricants. 2021; 9(9):93. doi: 10.3390/lubricants9090093

15. Dawood MA, Alasady ZMK, Abdulazeez MS, Ahmed DS, Sulaiman GM, Kadhum AAH, Shaker LM, Alamiery AA. The corrosion inhibition effect of a pyridine derivative for low carbon steel in 1 M HCl medium: Complemented with antibacterial studies. Int J Corros Scale Inhib. 2021; 10:1766-1782. doi: 10.17675/2305-6894-2021-10-4-25

16. Alamiery AA. Corrosion inhibition effect of 2-N-phenylamino-5-(3-phenyl-3-oxo-1-propyl)-1,3,4-oxadiazole on mild steel in 1 M HCl medium: Insight from gravimetric and DFT investigations. Mater Sci Energy Technol. 2021; 4:398-406. doi: 10.1016/j.mset.2021.09.002

17. Alamiery AA. Anticorrosion effect of thiosemicarbazide derivative on mild steel in 1 M HCl and 0.5 M sulfuric Acid: Gravimetrical and theoretical studies. Mater Sci Energy Technol. 2021; 4:263-273. doi: 10.1016/j.mset.2021.07.004

18. Alamiery AA, Isahak WNRW, Aljibori H, Al-Asadi H, Kadhum A. Effect of the structure, immersion time and temperature on the corrosion inhibition of 4-pyrrol-1-yln-(2,5-dimethyl-pyrrol-1-yl)benzoylamine in 1.0 m HCl solution. Int J Corros Scale Inhib. 2021; 10:700-713. doi: 10.17675/2305-6894-2021-10-2-14

19. Alamiery A, Mahmoudi E, Allami T. Corrosion inhibition of low-carbon steel in HCl environment using a Schiff base derived from pyrrole: gravimetric and computational studies. Int J Corros Scale Inhib. 2021; 10:749-765. doi: 10.17675/2305-6894-2021-10-2-17.

20. Eltmimi AJM, Alamiery A, Allami AJ, Yusop RM, Kadhum AH, Allami T. Inhibitive effects of a novel efficient Schiff base on mild steel in HCl environment. Int J Corros Scale Inhib. 2021; 10:634-648. doi: 10.17675/2305- 6894-2021-10-2-10

21. Alamiery A, Shaker LM, Allami T, Kadhum AH, Takriff MS. A study of acidic corrosion behavior of Furan-Derived Schiff base for mild steel in HCl environment: Experimental, and surface investigation. Mater Today: Proc. 2021; 44:2337-2341. doi: 10.1016/j.matpr.2020.12.431

22. Al-Baghdadi S, Al-Amiery A, Gaaz T, Kadhum A. Terephthalohydrazide and isophthalohydrazide as new

corrosion inhibitors for mild steel in HCl: Experimental and theoretical approaches. Koroze Ochr Mater. 2021; 65:12-22. doi: 10.2478/kom-2021-0002

23. Hanoon MM, Resen AM, Shaker LM, Kadhum A, Al-Amiery A. Corrosion investigation of mild steel in aqueous HCl environment using n- (Naphthalen-1yl)-1-(4-pyridinyl)methanimine complemented with antibacterial studies. Biointerface Res Appl Chem. 2021; 11:9735–9743. doi: 10.33263/BRIAC112.97359743

24. Al-Baghdadi S, Gaaz TS, Al-Adili A, Al-Amiery A, Takriff M. Experimental studies on corrosion inhibition performance of acetylthiophene thiosemicarbazone for mild steel in HCl complemented with DFT investigation. Int J Low-Carbon Technol. 2021; 16:181-188. doi: 10.1093/ijlct/ctaa050

25. Al-Amiery A. Anti-corrosion performance of 2-isonicotinoyl-n-phenylhydrazinecarbothioamide for mild steel HCl solution: Insights from experimental measurements and quantum chemical calculations. Surf Rev Lett. 2021; 28:2050058. doi: 10.1142/S0218625X20500584

26. Abdulazeez MS, Abdullahe ZS, Dawood MA, Handel ZK, Mahmood RI, Osamah S, et al. Corrosion inhibition of low carbon steel in HCl medium using a thiadiazole derivative: weight loss, DFT studies and antibacterial studies. Int J Corros Scale Inhib. 2021; 10:1812-1828. doi: 10.17675/2305-6894-2021-10-4-27

27. Mustafa A, Sayyid F, Betti N, Hanoon M, Al-Amiery A, Kadhum A, et al. Inhibition evaluation of 5-(4-(1H-pyrrol-1-yl)phenyl)-2-mercapto-1,3,4-oxadiazole for the corrosion of mild steel in an acid environment: thermodynamic and DFT aspects. Tribologia. 2021; 38:39-47. doi: 10.30678/fjt.105330

28. Abdulsahib YM, Eltmimi AJM, Alhabeeb SA, Hanoon MM, Al-Amiery AA, Allami T, et al. Experimental and theoretical investigations on the inhibition efficiency of N-(2,4-dihydroxytoluen-eylidene)-4-methylpyridin-2-amine for the corrosion of mild steel in HCl. Int J Corros Scale Inhib. 2021; 10:885-899. doi: 10.17675/2305-6894-2021-10-3-3

29. Khudhair AK, Mustafa AM, Hanoon MM, Al-Amiery A, Shaker LM, Gazz T, et al. Experimental and theoretical investigation on the corrosion inhibitor potential of N-MEH for mild steel in HCl. Prog. Color Colorant Coat. 2022; 15:111-122. doi: 10.30509/PCCC.2021.166815.1111

30. Zinad DS, Salim RD, Betti N, Shaker LM, Al-Amiery AA. Comparative investigations of the corrosion inhibition efficiency of a 1-phenyl-2-(1-phenylethylidene)hydrazine and its analog against mild steel corrosion in HCl solution. Prog. Color Colorant Coat. 2022; 15(1):5363. doi: 10.30509/pccc.2021.166786.1108

31. Aljibori HS, Abdulzahra OH, Al Adily AJ, Al-Azzawi WK, Al-Amiery AA and Kadhum AAH,

Recent progresses in thiadiazole derivatives as corrosion inhibitors in hydrochloric acid solution, Int J Corros Scale Inhib. 2023; 12(3):842-866. doi: 10.17675/2305-6894-2023-12-3-3

32. Rouin G, Abdelmouleh M, Mallah A, Masmoudi M. Oil extracted from spent coffee grounds as a green corrosion inhibitor for copper in a 3 wt. % NaCl solution. Coatings. 2023; 13(10):1745. https://doi.org/10.3390/coatings13101745.

33. Al-Sharabi HAA, Bouiti K, Bouhlal F, LabjarN,Anti-corrosive properties of Catha Edulis leaves extract on C38 steel in 1 M HCl media. Experimental and theoretical study. Inter J Corr Scale Inhib.2022; 11(3):956-984. doi:10.17675/2305-6894-2022-11-3-4

34. F. Bouhlal, A. Mazkour, H. Labjar, M. Benmessaoud, M. Serghini-Idrissi, M. El Mahia, El M. Lotfi, S. El Hajjaji, N. Labjar, Combination effect of hydro-alcoholic extract of spent coffee grounds (HECG) and potassium Iodide (KI) on the C38 steel corrosion inhibition in 1 M HCl medium: Experimental design by response surface methodology, Chem Data Collect. 2020; 29: 100499. doi: 10.1016/j.cdc.2020.100499

35. Dehghani A, Bahlakeh G, Ramezanzadeh B, Ramezanzadeh M, Potential of borage flower aqueous extract as an environmentally sustainable corrosion inhibitor for acid corrosion of mild steel: Electrochemical and theoretical studies. J Mol Liq. 2019; 277: 895-911. doi: 10.1016/j.molliq. 2019.01.008

36. Kang J, Wen J, Jayaram SH, Yu A, Wang X. Development of an equivalent circuit model for electrochemical double layer capacitors (EDLCs) with distinct electrolytes. Electrohim Acta. 2014; 115: 587-598. doi: 10.1016/j.electacta.2013.11.002

37. Muñoz AI, Antón J, Guiñón JL and Herranz VP, Inhibition effect of chromate on the passivation and pitting corrosion of a duplex stainless steel in LiBr solutions using electrochemical techniques. Corros Sci. 2007; 49: 3200-3225. doi: 10.1016/j.corsci.2007.03.002

38. Yea Y, Yang D, Chen H, Guo S, Yang Q, Chen L, Zhao H and Wangb L, A high-efficiency corrosion inhibitor of N-doped citric acid-based carbon dots for mild steel in hydrochloric acid environment. J Hazard Mater. 2020; 381:121019. doi: 10.1016/j.jhazmat.2019. 121019

39. Salim RD, Betti N, Hanoon M, Al-Amiery AA. 2-(2,4-Dimethoxybenzylidene)-N-phenylhydrazine-carbothioamide as an efficient corrosion inhibitor for mild steel in acidic environment. Prog Color Colorant Coat. 2021; 15:45-52. doi: 10.30509/pccc.2021.166775.1105.

40. Al-Amiery AA, Shaker LM, Kadhum AH, Takriff MS. Exploration of furan derivative for application as corrosion inhibitor for mild steel in HCl solution: Effect of immersion time and temperature on efficiency. Mater Today: Proc. 2021; 42:2968-2973. doi: 10.1016/j.matpr.2020.12.807

41. Resen AM, Hanoon MM, Shaker LM, Kadhum A, Al-Amiery A. Exploration of 8-piperazine-1-ylmethylumbelliferone for application as a corrosion inhibitor for mild steel in HCl solution. Int J Corros Scale Inhib. 2021; 10:368-387. doi: 10.17675/2305-6894-2021-10-1-21

42. Hanoon MM, Resen AM, Al-Amiery A, Kadhum AH, Takriff MS. Theoretical and experimental studies on the corrosion inhibition potentials of 2-((6-methyl-2-ketoquinolin-3-yl)methylene)hydrazinecarbothio-amide for mild steel in 1 M HCl. Prog Color Colorant Coat. 2021; 15(1): 11-23. doi: 10.30509/PCCC.2020.166739.1095

43. Hashim FG, Salman TA, Al-Baghdadi SB, Gaaz T, Al-Amiery AA. Inhibition effect of hydrazine-derived coumarin on a mild steel surface in HCl. Tribologia. 2020; 37: 45-53. doi: 10.30678/fjt.95510

44. Resen AM, Hanoon MM, Salim RD, Al-Amiery AA, Shaker LM, Kadhum AA. Gravimetrical, theoretical, and surface morphological investigations of corrosion inhibition effect of 4-(benzoimidazole-2-yl)pyridine on mild steel in HCl. Koroze Ochr Mater 2020; 64:122-130. doi: 10.2478/kom-2020- 0018

45. Salman AZ, Jawad QA, Ridah KS, Shaker LM, Al-Amiery AA. Selected BISthiadiazole: synthesis and corrosion inhibition studies on mild steel in HCl Environment. Surf Rev Lett. 2020; 27: 2050014. doi: 10.1142/S0218625X20500146

46. Junaedi S, Al-Amiery A, Kadihum A, Kadhum A, Mohamad A. Inhibition effects of a synthesized novel 4-aminoantipyrine derivative on the corrosion of mild steel in HCl solution together with quantum chemical studies. Int J Mol Sci. 2013; 14:11915-11928. doi: 10.3390/ijms140611915

47. Annon IA, Abbas AS, Al-Azzawi WK, Hanoon MM, Alamiery AA, Isahak WNRW, Kadhum AAH, Corrosion inhibition of mild steel in hydrochloric acid environment using thiadiazole derivative: Weight loss, thermodynamics, adsorption and computational investigations. S Afr J Chem Eng. 2022; 41: 244-252. doi: 10.1016/j.sajce.2022.06.011

48. Al-Baghdadi S, Hashim F, Salam A, Abed T, Gaaz T, Al-Amiery A, et al. Synthesis and corrosion inhibition application of NATN on mild steel surface in acidic media complemented with DFT studies. Results Phys. 2018; 8:1178-1184. doi: 10.1016/j.rinp.2018.02.007

49. Al-Azzawi WK, Al Adily AJ, Sayyid FF, Al-Azzawi RK, Kzar MH, Jawoosh HN, et al. Evaluation of corrosion inhibition characteristics of an N-propionanilide derivative for mild steel in 1 M HCl: Gravimetrical and computational studies. Int J Corros Scale Inhib. 2022; 11:1100-1114. doi: 10.17675/2305-6894-2022-11-3-12

50. Al-Amiery AA, Isahak WNRW, Al-Azzawi WK. Corrosion inhibitors: natural and synthetic organic inhibitors. Lubricants. 2023; 11:174. doi:10.3390/lubricants11040174

51. Betti N, Al-Amiery AA, Al-Azzawi WK, Isahak WNRW. Corrosion inhibition properties of Schiff base derivative against mild steel in HCl environment complemented with DFT investigations. Sci Reports. 2023; 13:8979. doi: 10.1038/s41598-023-36064-w

52. Al-Amiery A, Isahak WNRW, Al-Azzawi WK. ODHI: A Promising isatin-based corrosion inhibitor for mild steel in HCl. J Mol Struct. 2023; 1288: 135829. doi: https://doi.org/10.1016/j.molstruc.2023.135829.

53. Al-Amiery AA, Betti N, Isahak WNRW, Al-Azzawi WK, Wan Nik WMN. Exploring the effectiveness of isatin–schiff base as an environmentally friendly corrosion inhibitor for mild steel in HCl. Lubricants. 2023; 11:211. doi:10.3390/lubricants11050211.

54. Al-Edan AK, Isahak WNRW, Che Ramli ZA, Al-Azzawi WK, Kadhum AAH, Jabbar HS. et al. Palmitic acid-based amide as a corrosion inhibitor for mild steel in 1M HCl. Heliyon. 2023; 9:e08625. doi: 10.1016/j.heliyon.2023.e14657

55. Naseef Jasim A, Abdulhussein BA, Mohammed Noori Ahmed S, Al-Azzawi WK, Hanoon MM, Abbass MK, Al-Amiery AA. Schiff's base performance in preventing corrosion on mild steel in acidic conditions. Prog Color Colorant Coat. 2023; 16(4):319-29. doi: 10.30509/pccc.2023.167081.1197

56. Mohammed A, Rubaye AY, Al-Azzawi WK, Alamiery A. Investigation of the corrosion inhibition properties of 4-cyclohexyl-3-thiosemicarbazide on mild steel in 1 M HCl solution. Prog Color Colorant Coat. 2023; 16(4):347-59. doi: 10.30509/PCCC.2023.167126.1212

57. Hussein SS, Al-Hasani IDD, Abed AM, Hanoon MM, Shaker LM, Al-Amiery A, et al. Antibacterial corrosion inhibitor for the protection of mild steel in 1 M HCl solution. Prog Color Colorant Coat. 2023; 16:59-70. doi: 10.30509/pccc.2022.166935.1149

58. Raheef KM, Qasim HS, Radhi AA, Al-Azzawi WK, Hanoon MM, Al-Amiery AA. Gravimetric and density functional theory investigations on 4-aminoantipyrin schiff base as an inhibitor for mild steel in HCl solution. Progress Color Colorant Coat. 2023; 16:255-269. doi: 10.30509/PCCC.2023.167077.1196

59. Alamiery A. Case study in a conceptual DFT investigation of new corrosion inhibitor. Lett Appl NanoBioSci. 2021; 11:4007-4015. doi: 10.33263/LIANBS114.40074015

60. Alamiery A. Effect of temperature on the corrosion inhibition of 4-ethyl-1-(4-oxo-4-phenylbutanoyl) thiosemicarbazide on mild steel in HCl solution. Lett Appl NanoBioSci. 2022; 11:3502-3508. doi:10. 33263/LIANBS112.35023508

61. Betti N, Al-Azzawi WK, Alamiery A. Synthesis and study of corrosion behavior of terephthalaldehyde-derived schiff base for low-carbon steel in HCl: experimental, morphological and theoretical investigation. KOM–Corr Mater Protect J. 2022; 66:103-112.

62. Carranza MS, Reyes YI, Gonzales EC, Arcon DP, Franco FC. Electrochemical and quantum mechanical investigation of various small molecule organic

compounds as corrosion inhibitors in mild steel. Heliyon. 2021; 7(9):17-26.

63. Khadom AA, Mahmmod AA. Quantum chemical and mathematical statistical calculations of phenyltetrazole derivatives as corrosion inhibitors for mild steel in acidic solution: a theoretical approach. Result Eng. 2022; 16:100741.

64. Malinowski S, Wróbel M, Woszuk A. Quantum chemical analysis of the corrosion inhibition potential by aliphatic amines. Materials. 2021; 14(20):6197.

65. Boulechfar C, Ferkous H, Delimi A, Berredjem M, Kahlouche A, Madaci A, Djellali S, Boufas S, Djedouani A, Errachid A, Khan AA. Corrosion inhibition of Schiff base and their metal complexes with [Mn (II), Co (II) and Zn (II)]: Experimental and quantum chemical studies. J Mol Liq. 2023; 378:121637.

66. Punitha N, Sundaram RG, Vengatesh G, Rengasamy R, Elangovan J. Bis-1,2,3-triazole derivative as an efficient corrosion inhibitor for mild steel in hydrochloric acid environment: Insights from experimental and computational analysis. Inorg Chem Commun. 2023; 153:110732.

67. ASTM International, Standard Practice for Preparing, Cleaning, and Evaluating Corrosion Test, 2011, 1–9.

68. NACE International, Laboratory Corrosion Testing of Metals in Static Chemical Cleaning Solutions at Temperatures below 93°C (200°F), TM0193-2016-SG, 2000

69. Gaussian 03, Revision B.05. Gaussian, Inc., Wallingford, CT, 2004.

70. Koopmans T. Ordering of wave functions and eigen-energies to the individual electrons of an atom. Physica. 1934;1(1-6):104-113. doi: 10.1016/S0031-8914(34)90011-2

71. Betti N, Al-Amiery A. Corrosion inhibition screening of 2-((6-aminopyridin-2-yl)imino)indolin-3-one: weight loss, morphology, and DFT investigations. Corr Sci Technol. 2023; 22(1): 10-20. doi: 10.14773/CST.2023.22.1.10

72. Mahdi BS, Abbass MK, Mohsin MK, Al-Azzawi WK, Hanoon MM, AlKaabi MHH, Shaker LM, Al-Amiery AA, Isahak WNRW, Kadhum AAH, Takriff MS. Corrosion inhibition of mild steel in hydrochloric acid environment using terephthaldehyde based on Schiff base: Gravimetric, thermodynamic, and computational studies. Molecules. 2022; 27(15):4857. doi: 10.3390/molecules27154857 142.

73. Jawad QA, Zinad DS, Salim RD, Al-Amiery AA, Gaaz TS, Takriff MS, Kadhum AAH. Synthesis characterization, and corrosion inhibition potential of novel thiosemicarbazone on mild steel in sulfuric acid environment. Coatings. 2019; 9(11): 729. doi: 10.3390/coatings9110729.

74. Abbas AS, Mahdi BS, Abbas HH, Sayyid FF, Mustafa AM, Annon IA, Abdulsahib YM, Resen AM, Hanoon MM, Obaeed NH. Corrosion behavior optimization by nanocoating layer for low carbon seel

75. Sayyid FF, Mustafa AM, Hanoon MM, Saker LM, Alamiery AA. Corrosion protection effectiveness and adsorption performance of schiff base-quinazoline on mild steel in HCl environment. Corr Sci Technol. 2022; 21(4): 77-88. doi: 10.14773/CST.2022.21.2.77

76. Al-Amiery A, Shaker LM, Kadhum AAH, Takriff MS. Synthesis, characterization and gravimetric studies of novel triazole-based compound. Int J LowCarbon Technol. 2020; 15(2):164-170. doi: 10.1093/ijlct/ctz067.

77. Mustafa AM, Abdullahe ZS, Sayyid FF, Hanoon MM, Al-Amiery AA, Isahak WN. 3-Nitrobenzaldehyde-4-phenylthiosemicarbazone as active corrosion inhibitor for mild steel in a hydrochloric acid environment. Prog Color Colorant Coat. 2022; 15(4):285-93. doi: 10.30509/PCCC.2021.166869.1127

78. Abbass MK, Raheef KM, Aziz IA, Hanoon MM, Mustafa AM, Al-Azzawi WK, Al-Amiery AA, Kadhum AAH, Evaluation of 2-dimethyl-aminopropionamidoantipyrine as a corrosion inhibitor for mild steel in HCl solution: A combined experimental and theoretical study, Progress Color Colorant Coat. 2024; 17: 1-10. doi: 10.30509/pccc.2023.167081.1197

79. Shanmugapriya R, Ravi M, Ravi S, Ramasamy M, Maruthapillai A. Electrochemical and Morphological investigations of Elettaria cardamomum pod extract as a green corrosion inhibitor for Mild steel corrosion in 1 N HCl. Inorg Chem Commun. 2023; 154:110958. doi: 10.1016/j.inoche.2023.110958

80. Al-Amiery AA, Al-Azzawi WK. Organic synthesized inhibitors for corrosion protection of carbon steel: A comprehensive review. J Bio Tribo Corr. 2023; 9(4):74. doi: 10.1007/s40735-023-00791-4

81. Abtan NS, Al-Hamid MAI, Kadhim LA, Sayyid FA, Noori FTM, Kadum A, Alamiery A, AlAzzawi WK. Unlocking the power of 4-acetamidoantipyrine: a promising corrosion inhibitor for preserving mild steel in harsh hydrochloric acid Eenvironments. Prog Color Colorant Coat. 2024; 17(1):85-96. doi: 10.30509/pccc.2023.167147.1223.

82. Méndez-Figueroa H, Colorado-Garrido D, Hernández-Pérez M, Galván-Martínez R, Cruz RO. Neural networks and correlation analysis to improve the corrosion prediction of SiO_2-nanostructured patinated bronze in marine atmospheres. J Electroanal Chem. 2022; 917:116396.

83. Xu L, Wang Y, Mo L, Tang Y, Wang F, Li C. The research progress and prospect of data mining methods on corrosion prediction of oil and gas pipelines. Eng Fail Anal. 2022; 17:106951.

84. Wang L, Wang H, Seyeux A, Zanna S, Pailleret A, Nesic S, Marcus P. Adsorption mechanism of quaternary ammonium corrosion inhibitor on carbon steel surface using ToF-SIMS and XPS. Corr Sci. 2023; 213:110952.

85. Wang DY, Wang JH, Li HJ, Wu YC. Pectin-amino acid derivatives as highly efficient green inhibitors for the corrosion of N80 steel in CO₂-saturated formation water. Indust Crops Prod. 2022; 189:115866.

86. Sharifi A, Miri R, Riazi M. A holistic review of harsh conditions resistant surfactants for enhanced oil recovery in dense carbonate reservoir. Fuel. 2023; 353:129109.

87. Aslam R, Serdaroglu G, Zehra S, Verma DK, Aslam J, Guo L, Verma C, Ebenso EE, Quraishi MA. Corrosion inhibition of steel using different families of organic compounds: Past and present progress. J Mol Liq. 2022; 348:118373.

88. Raviprabha K, Bhat RS. Corrosion inhibition of mild steel in 0.5 M HCl by substituted 1, 3, 4-oxadiazole. Egy J Pet. 2023; 32(2):1-10.

89. Sharma D, Thakur A, Sharma MK, Sharma R, Kumar S, Sihmar A, Dahiya H, et al. Effective corrosion inhibition of mild steel using novel 1, 3, 4-oxadiazole-pyridine hybrids: Synthesis, electrochemical, morphological, and computational insights. Environ Res. 2023; 234:116555.

90. Kumar S, Kalia V, Kumar P, Kumar S, Goyal M, Pahuja P, Jhaa G, Lata S, et al. Synthesis, characterization and corrosion inhibition potential of oxadiazole derivatives for mild steel in 1M HCl: electrochemical and computational studies. J Mol Liq. 2022;348:118021.

91. Rezaeivala M, Bozorg M, Rafiee N, Sayin K, Tuzun B. Corrosion inhibition of Carbon Steel using a new morpholine-based ligand during acid pickling: Experimental and theoretical studies. Inorg Chem Commun. 2023; 148:110323.

92. Abdallah M, Al-Habal T, El-Sayed R, Awad MI, Abdel Hameed RS. Corrosion control of carbon steel in acidic media by nonionic surfactant compounds derived from 1,3,4-Oxadiazole and 1,3,4-Thiadiazole. Inter J Electrochem Sci. 2022; 17(12):221255.

93. Tanwer, S. Kumar Shukla, S. Cefuroxime: A potential corrosion inhibitor for mild steel in sulphuric acid medium. Prog. Color Colorant Coat. 2023; 16:125-138.

94. Chaouiki A, Chafiq M, Al-Moubaraki AH, Bakhouch M, El Yazidi M, Ko YG. Electrochemical behavior and interfacial bonding mechanism of new synthesized carbocyclic inhibitor for exceptional corrosion resistance of steel alloy: DFTB, MD and experimental approaches. Arab J Chem. 2022; 15(12):104323.

95. Wang W, Kang R, Yin Y, Tu S, Ye L. Two-step pyrolysis biochar derived from agro-waste for antibiotics removal: mechanisms and stability. Chemosphere. 2022; 292:133454.

96. Loganathan M, Raj AS, Murugesan A, Kumar PS. Effective adsorption of crystal violet onto aromatic polyimides: Kinetics and isotherm studies. Chemosphere. 2022; 304:135332.

97. Qiu M, Liu L, Ling Q, Cai Y, Yu S, Wang S, Fu D, Hu B, Wang X. Biochar for the removal of contaminants from soil and water: a review. Biochar. 2022; 4(1):19.

98. Raghav L, Patanjali P, Patanjali N, Singh R. Adsorption of malachite green and chrysoidine-Y by Sn-pillared clay. Environ Qual Manage. 2023; 32(3):181-193.

99. Udoh TH, Sunday MU. Investigation of corrosion inhibition potential of selected biological inhibitors. Niger J Technol. 2022; 41(2):263-269.

100. Danhassan UA, Zhang X, Qi R, Ali MM, Sheng K, Lin H. Nickel-Catalyzed mesoporous biochar for enhanced adsorptive oxidation of aqueous Sulfide: An investigation of influencing factors and mechanisms. Bioresour Technol. 2022; 362:127877.

101. Viet NM, Hoai PT, Huong NTM. Porous adsorbent derived from acid activation of food waste biochar: A sustainable approach for novel removal chlorophenol in wastewater. Environ Res. 2023; 216:114735.

102. Luo Y, Han Y, Hua Y, Xue M, Yu S, Zhang L, Yin Z, et al. Step scheme nickel-aluminium layered double hydroxides/biochar heterostructure photocatalyst for synergistic adsorption and photodegradation of tetracycline. Chemosphere. 2022; 309:136802.

103. Ogunyemi BT, Ojo FK. Corrosion inhibition potential of thiosemicarbazide derivatives on aluminium: Insight from Molecular Modelling and QSARS approaches. J Nigerian Soc Phys Sci. 2023:915-915.

104. Oyeneyin OE, Ojo ND, Ipinloju N, Agbaffa EB, Emmanuel AV. Investigation of corrosion inhibition potentials of some 2-(4-(substituted) arylidene)-1H-indene-1, 3-dione derivatives: density functional theory and molecular dynamics simulation. Beni-Suef Univ J Basic Appl Sci. 2022; 11(1):1-14.

105. Iorhuna F, Thomas NA, Lawal SM. A Theoretical properties of Thiazepine and its derivatives on inhibition of Aluminium Al (110) surface. Algerian J Eng Technol. 2023; 8(1):43-51.

106. Oyeneyin OE, Ojo ND, Ipinloju N, Akinwumi ACJ, Agbaffa EB. Investigation of corrosion inhibition potentials of some aminopyridine schiff bases using density functional theory and Monte Carlo simulation. Chem Africa. 2022; 5(2):319-332.

107. Karaoui M, Zarrouk AM, Hsissou R, Alami M, Assouag M. Performance of organic molecules as corrosion inhibitors for CS: a comprehensive review. Anal Bioanal Electrochem. 2022; 14(6):535-556.

108. Wani TA, Zargar S. Molecular Spectroscopy Evidence of 1, 3, 5-Tris (4-carboxyphenyl) benzene binding to DNA: anticancer potential along with the comparative binding profile of intercalation via modeling studies. Cells. 2023; 12(8):1120.

109. Ejaz SA, Farid A, Zargar S, Channar PA, Aziz M, Wani TA, Attaullah HM, et al. Computational and theoretical chemistry of newly synthesized and characterized 2, 2'-(5, 5'-(1, 4-phenylene) bis (1 H-tetrazole-5, 1-diyl)) bis-N-acetamides. BMC Chem. 2023; 17(1):97.

110. Chraka A, Akroujai EH, Chetioui S, Benzbiria N, Barrahi A, Chraka A, Djedouani A, et al. Int J Corr Scale Inhib. 2023; 12(3):1102-1135.

111. Bui TQ, Thoi BT, Nguyen PDN, Thao TPPT, Chien TV, Loc TV, Nhung NTA. In silico screening for inhibitory potentiality towards protein structure tyrosine phosphatase 1B of sulfonylureas derivatives. Vietnam J Chem. 2022; 60(1):123-132.

112. Iorhuna F, Nyijime AT, Ayuba AM. 2-Phenylpiperazine, N, N'-di-TFA as a corrosion inhibitor: A computational comparative study on the Aluminium and Zinc surface. Moroccan J Chem. 2023; 11(3):11-3.

113. Mamand DMM, Awla AH, Al-Ahmad AJT, Aziz HAA, Al-Soudani M, Kadir MFZ. Novel pyridinium-based ionic liquids as potential corrosion inhibitors for mild steel: electrochemical and DFT studies. J Mol Liq. 2022; 16: 355:

114. Iorhuna F, Muhammad ASM, Ayuba AM, Nyijime AT. Molecular dynamic simulations and quantum chemical studies of nitrogen based heterocyclic compounds as corrosion inhibitors on mild steel surface. Chem Rev Lett. 2023; 6(2):114-127.

115. Shattle EE, Elshawi ZM, Khalil SM, Erteeb MA, Eldrhube TM. Theoretical Studies on allylphenylphosphonium halides as corrosion inhibitors for Iron metal. Am J Chem. 2023; 13(2):36-41.

116. Zakaria K, Abbas MA, Bedair MA. Herbal expired drug bearing glycosides and polysaccharides moieties as green and cost-effective oilfield corrosion inhibitor: Electrochemical and computational studies. J Mol Liquids. 2022; 352:118689.

117. Mazlan N, Jumbri K, Kassim MA, Wahab RA, Rahman MBA. Density functional theory and molecular dynamics simulation studies of bio-based fatty hydrazide-corrosion inhibitors on Fe (110) in acidic media. J Mol Liquids. 2022; 347:118321.

118. Rasul HH, Mamad DM, Azeez YH, Omer RA, Omer KA. Theoretical investigation on corrosion inhibition efficiency of some amino acid compounds. Comput Theor Chem. 2023; 114177.

119. Al-Qurashi OS, Wazzan N. Molecular and periodic DFT calculations of the corrosion protection of Fe (110) by individual components of aerva lanata flower as a green corrosion inhibitor. J Saudi Chem Soc. 2022; 26(6):101566.

120. Murmu M, Murmu NC, Ghosh M, Banerjee P. Density functional theory, Monte Carlo simulation and non-covalent interaction study for exploring the adsorption and corrosion inhibiting property of double azomethine functionalized organic molecules. J Adhes Sci Technol. 2022; 36(23-24):2732-2760.

121. Auepattana-Aumrung K, Crespy D. Self-healing and anticorrosion coatings based on responsive polymers with metal coordination bonds. Chem Eng J. 2023; 452:139055.

122. Chen S, Xue Y, Peng L, Li H, Lei Y, Huang Z, Jiao J. Research progress on types and mechanism of common organic corrosion inhibitors. Int J Energy. 2023; 2(3):9-12.

123. Medimagh M, Issaoui N, Gatfaoui S, Kazachenko AS, Al-Dossary OM, Kumar N, Marouani H, Bousiakoug LG. Investigations on the non-covalent interactions, drug-likeness, molecular docking and chemical properties of 1,1,4,7,7-pentamethyldiethylenetriammonium trinitrate by density-functional theory. J King Saud Univ-Sci. 2023; 35(4):102645.

124. Alizada A, Arslan H. Experimental and theoretical studies of a thiourea derivative: 1-(4-chloro-benzoyl)-3-(2-trifluoromethyl-phenyl) thiourea. J Mol Struct. 2023; 1279:134996.

125. El Bakri Y, Kurbanova M, Ahsin A, Ramazanzade N, Al-Salahi R. A probe to surface reactivity, crystal structure, and DFT investigations for newly synthesized 4,5-bis (4-Nitrophenyl)-8a-phenyl-decahydro-[1, 3] diazino [4, 5-d] pyrimidine-2, 7-dione: a combined theoretical and experimental study. Crystals. 2023; 13(6):942.

126. Venugopal PP, Kumari PDR, Chakraborty D. Anti-corrosion investigation of a new nitro veratraldehyde substituted imidazopyridine derivative Schiff base on mild steel surface in hydrochloric acid medium: Experimental, computational, surface morphological analysis. Mater Chem Phys. 2022; 281:125855.

127. Keskin E, Arslan H. Synthesis, crystal structure, DFT calculations, and Hirshfeld surface analysis of an NNN pincer type compound. J Mol Struct. 2023; 1283:135252.

128. Zakaria K, Abbas MA, Bedair MA. Herbal expired drug bearing glycosides and polysaccharides moieties as green and cost-effective oilfield corrosion inhibitor: Electrochemical and computational studies. J Mol Liquids. 2022; 352:118689.

129. Jrajri K, El Faydy M, Benhiba F, Al Garadi W, El Ghayati L, Sebbar NK, Essassi EM, et al. Some diazepinone analogs as corrosion inhibitors for carbon steel in a hydrochloric acid medium: An integrated theoretical and practical study. Mater Today Commun. 2023; 36:106673.

130. Olasehinde EF, Agbaffa EB, Adebayo MA, Abata EO. Corrosion inhibition of mild steel in 1 M HCl by methanolic chromolaena odorata leaf extract: experimental and theoretical studies. J Bio-and Tribo-Corrosion. 2022; 8(4):105.

131. Chiter F, Costa D, Pébère N, Marcus P, Lacaze-Dufaure C. Insight at the atomic scale of corrosion inhibition: DFT study of 8-hydroxyquinoline on oxidized aluminum surfaces. Phys Chem Chem Phys. 2023; 25(5):4284-4296.

132. Li Y, Xu W, Li H, Lai J, Qiang S. Corrosion inhibition mechanism of Xanthium sibiricum inhibitor and its comprehensive effect on concrete performance: experimental analysis and theoretical calculation. Constr Build Mater. 2022; 348:128672.

133. Hernández-Bravo R, Miranda AD, Parra JG, Alvarado-Orozco JM, Domínguez-Esquivel JM,

Mujica V. Experimental and theoretical study on the effectiveness of ionic liquids as corrosion inhibitors. Comput Theor Chem. 2022; 1210:113640.

134. Oyeneyin OE, Ojo ND, Ipinloju N, Agbaffa EB, Emmanuel AV. Investigation of the corrosion inhibition potentials of some 2-(4-(substituted) arylidene)-1H-indene-1, 3-dione derivatives: density functional theory and molecular dynamics simulation. Beni-Suef Univ J Basic Appl Sci. 2022; 11(1):1-14.

135. Mandal S, Zamindar S, Sarkar S, Murmu M, Guo L, Kaya S, Hirani H, Banerjee P. Quantum chemical and molecular dynamics simulation approach to investigate adsorption behaviour of organic azo dyes on TiO_2 and ZnO surfaces. J Adhes Sci Technol. 2023; 37(10):1649-1665.

136. Alghamdi SK, Abbas F, Hussein RK, Alhamzani AG, El-Shamy NT. Spectroscopic characterization (IR, UV-Vis), and HOMO-LUMO, MEP, NLO, NBO analysis and the antifungal activity for 4-bromo-N-(2-nitrophenyl) benzamide; using DFT modeling and In silico molecular docking. J Mol Struct. 2023; 1271:134001.

137. Díaz-Jiménez V, Arellanes-Lozada P, Likhanova NV, Olivares-Xometl O, Chigo-Anota E, Lijanova IV, Gómez-Sánchez G, Verpoort F. Investigation of sulfonium-iodide-based ionic liquids to inhibit corrosion of API 5L X52 steel in different flow regimes in acid medium. ACS Omega. 2022; 7(47):42975-42993.

138. Akinyele OF, Adekunle ASA, Olayanju DS, Oyeneyin OE, Durodola SS, Ojo ND, Akinmuyisitan AA, Ajayeoba TA, Olasunkanmi LO. Synthesis and corrosion inhibition studies of (E)-3-(2-(4 chloro-2-nitrophenyl) diazenyl)-1-nitrosonaphthalen-2-ol on mild steel dissolution in 0.5 M HCl solution-experimental, DFT and Monte Carlo Simulations. J Mol Struct. 2022;1268:133738.

139. Alimohammadi M, Ghaderi M, Ramazani SA, Mahdavian M. Falcaria vulgaris leaves extract as an eco-friendly corrosion inhibitor for mild steel in hydrochloric acid media. Sci Rep. 2023; 13(1):3737.

140. Ghaderi M, Ramazani SA, Kordzadeh A, Mahdavian M, Alibakhshi E, Ghaderi A. Corrosion inhibition of a novel antihistamine-based compound for mild steel in hydrochloric acid solution: Experimental and computational studies. Sci Rep. 2022;12(1):13450.

141. Ravi S, Peters S, Varathan E, Ravi M. Molecular interaction and corrosion inhibition of benzophenone and its derivative on mild steel in 1 N HCl: Electrochemical, DFT and MD simulation studies. Colloid Surf A. 2023; 661:130919.

142. Jasim ZI, Rashid KH, AL-Azawi KF, Khadom AA. Synthesis of schiff-based derivative as a novel corrosion inhibitor for mild steel in 1 M HCl solution: optimization, experimental, and theoretical investigations. J Bio-and Tribo-Corrosion. 2023; 9(3):54.

143. Kaya F, Solmaz R, Gecibesler IH. Adsorption and corrosion inhibition capability of Rheum ribes root extract (Işgın) for mild steel protection in acidic medium: A comprehensive electrochemical, surface characterization, synergistic inhibition effect, and stability study. J Mol Liquids. 2023; 372:121219.

144. Kaghazchi L, Naderi R, Ramezanzadeh B. Improvement of the dual barrier/active corrosion inhibition function of the epoxy composite filled with zinc-doped phytic acid-modified graphene oxide nanosheets. Prog Org Coat. 2022; 168:106884.

145. Zhong F, He Y, Wang P, Chen C, Wu Y. Novel pH-responsive self-healing anti-corrosion coating with high barrier and corrosion inhibitor loading based on reduced graphene oxide loaded zeolite imidazole framework. Colloids Surf A. 2022; 642:128641.

146. Mirzaei-Saatlo M, Jamali H, Moradi-Alavian S, Asghari E, Teimuri-Mofrad R, Esrafili MD. 4-Ferrocenylbutyl-based corrosion inhibitors for mild steel in acidic solution. Mater Chem Phys. 2023; 293:126895.

147. Fan B, Zhao X, Liu Z, Xiang Y, Zheng X. Inter-component synergetic corrosion inhibition mechanism of Passiflora edulia Sims shell extract for mild steel in pickling solution: experimental, DFT and reactive dynamics investigations. Sustain Chem Pharm. 2022; 29:100821.

148. Mahdy A, Aly KI, Mohamed MG. Construction novel polybenzoxazine coatings exhibiting corrosion protection of mild steel at different concentrations in a seawater solution. Heliyon. 2023; 9(7).

149. Bedair MA, Elaryian HM, Gad ES, Alshareef M, Bedair AH, Aboushahba RM, Fouda AES. Insights into the adsorption and corrosion inhibition properties of newly synthesized diazinyl derivatives for mild steel in hydrochloric acid: synthesis, electrochemical, SRB biological resistivity and quantum chemical calculations. RSC Adv. 2023; 13(1):478-498.

150. Bedair MA, Abuelela AM, Alshareef M, Owda M, Eliwa EM. Ethyl ester/acyl hydrazide-based aromatic sulfonamides: facile synthesis, structural characterization, electrochemical measurements and theoretical studies as effective corrosion inhibitors for mild steel in 1.0 M HCl. RSC Adv. 2023; 13(1):186-211.

151. El-Mokadem TH, Hashem AI, Abd El-Sattar NEA, Dawood EA, Abdelshafi NS. Green synthesis, electrochemical, DFT studies and MD simulation of novel synthesized thiourea derivatives on carbon steel corrosion inhibition in 1.0 M HCl. J Mol Struct. 2023; 1274:134567.

152. Zhang W, Wang S, Guo Z, Luo J, Zhang C. Heterocyclic group end-capped polyethylene glycol: Synthesis and used as corrosion inhibitors for mild steel in HCl medium. J Mol Liquids. 2023; 122779.

153. Aly KI, Amer AA, Mahross MH, Belal MR, Soliman AMM, Mohamed MG. Construction of novel polybenzoxazine coating precursor exhibiting

excellent anti-corrosion performance through monomer design. Heliyon. 2023; 9(5).

154. Yousef TA, Alhamzani AG, Abou-Krisha MM, Pradeep Kumar CB, Raghu MS, Yogesh Kumar K, Prashanth MK, Jeon BH. Experimental and theoretical examinations of triazole linked saccharin derivatives as organic corrosion inhibitors for mild steel in hydrochloric acid. J Mol Struct. 2023; 1275:134603.

155. Haque J, Saleh TA, Murmu M, Chauhan DS, Wan Nik WB, Banerjee P, Quraishi MA. Synthesis of multi donating sites grafted on graphene oxide nanosheets: Anti-corrosion study for mild steel in 1M HCl with DFT calculations. J Mol Liquids. 2023; 122820.

156. Abbas MA, Arafa EI, Bedair MA, Ismail AS, El-Azabawy OE, Baker SA, Al-Shafey HI. Synthesis, characterization, thermodynamic analysis and quantum chemical approach of branched N, N′-bis (p-hydroxybenzoyl)-based propanediamine and triethylenetetramine for carbon steel corrosion inhibition in hydrochloric acid medium. Arab J Sci Eng. 2023; 48(6):7463-7484.

157. Rashid KH, AL-Azawi KF, Khadom AA, Jasim AS, Kadhim MM. New pyrazole derivative as effective corrosion inhibitor for carbon steel in 1 M HCl: Experimental and theoretical analysis. J Mol Struct. 2023; 1287:135661.

158. Soliman AMM, Aly KI, Mohamed MG, Amer AA, Belal MR, Abdel-Hakim M. Synthesis, characterization and protective efficiency of novel polybenzoxazine precursor as an anticorrosive coating for mild steel. Sci Rep. 2023; 13(1):5581.

159. Gupta SK, Mehta RK, Kumari S, Yadav M, Obot IB. Study on benzylidine derivatives as corrosion inhibitors for mild steel in 15 % HCl medium: Experimental & theoretical investigation. J Phys Chem Solids. 2023; 111632.

160. Abdelhadi RA, Ahmed ZE, Abouzeid AM. Synthesis, spectroscopic analysis and electrochemical studies of novel organic compound based on N-alkylphthalazinone chemistry as corrosion inhibitor for carbon steel in 1M HCl. Int J Electrochem Sci. 2023; 18(5):100121.

161. Jasim ZI, Rashid KH, AL-Azawi KF, Khadom AA. New pyrazole derivative as effective corrosion inhibitor for carbon steel in 1 M HCl: experimental and theoretical analysis. J Mol Struct. 2023; 1287:135661.

162. Mehta RK, Gupta SK, Kumari N, Yadav M, Obot IB. Synthesized novel carbon dots as green corrosion inhibitor for mild steel in hydrochloric acid: Gravimetric, electrochemical and morphological studies. Diamond Relat Mater. 2023; 136:109992.Top of Form.